

Simulating quantum chaos on a quantum computer

Amit Anand^{1,3,4}, Sanchit Srivastava^{2,3,4}, Sayan Gangopadhyay^{3,4}, and Shohini Ghose^{4,5}

¹Department of Mechanical Engineering, Indian Institute of Engineering Science And Technology, Shibpur, Howrah-711103, West Bengal, India.

²School of Physics, Indian Institute of Science Education and Research, Thiruvananthapuram - 695551, Kerala, India

³Department of Physics and Astronomy, University of Waterloo, Waterloo, Ontario, Canada N2L 3G1

⁴Institute for Quantum Computing, University of Waterloo, Waterloo, Ontario, Canada N2L 3G1

⁵Department of Physics and Computer Science, Wilfrid Laurier University, Waterloo, Ontario, Canada N2L 3C5

Abstract

We show that currently available noisy intermediate-scale quantum (NISQ) computers can be used for versatile quantum simulations of chaotic systems. We introduce a novel classical-quantum hybrid approach for exploring the dynamics of the chaotic quantum kicked top (QKT) on a universal quantum computer. The programmability of this approach allows us to experimentally explore the complete range of QKT chaoticity parameter regimes inaccessible to previous studies. Furthermore, the number of gates in our simulation does not increase with the number of kicks, thus making it possible to study the QKT evolution for arbitrary number of kicks without fidelity loss. Using a publicly accessible NISQ computer (IBMQ), we observe periodicities in the evolution of the 2-qubit QKT, as well as signatures of chaos in the time-averaged 2-qubit entanglement. We also demonstrate a connection between entanglement and delocalization in the 2-qubit QKT, confirming theoretical predictions.

1 Introduction

The seeds that grew into the field of quantum computing were initially sown in the context of quantum simulations[1, 2]. As Feynman pointed out[3], the possibility of mapping one quantum system into another opens up new windows for efficiently exploring the properties and dynamics of general quantum systems[4, 5]. Large-scale, programmable quantum computers could offer exactly this type of possibility of mapping and simulating complex quantum systems[6]. While such large-scale quantum computers do not yet exist, it is worth exploring the potential for quantum simulations using currently available noisy intermediate-scale quantum (NISQ) computers[7, 8]. One such potential area of NISQ application is the topic of quantum chaos - the study of quantum systems that exhibit chaos in some classical limit. The question of how classical chaos emerges from quantum dynamics remains one of the open fundamental questions in quantum theory[9, 10, 10, 11]. On the experimental side as well, the quantum control and precision needed to explore quantum chaotic dynamics over a wide range of parameters and long time scales remains quite challenging. So far, relatively few experiments in limited parameter regimes and for short times have been performed[12, 13, 14, 15, 16]. In this work, we demonstrate the use of NISQ computers for flexible simulations of quantum chaos.

Classical chaos is characterized by exponential sensitivity to initial conditions quantified by the Lyapunov exponent that is a measure of the rate of divergence of neighbouring trajectories [17, 18, 19]. A corresponding quantum measure of chaos is challenging to define due to the uncertainty principle and the linearity of quantum evolution. In recent years, the question of quantum-classical correspondence in classically chaotic systems has been explored in the context of quantum information processing. The connection between fundamentally quantum phenomena such as entanglement and classical chaos has puzzled physicists for decades, and has

gained new relevance for quantum computing applications. It has been shown that classical chaos can affect the implementation of quantum computing algorithms [20, 21]. Chaos can also affect the generation of dynamical entanglement, an important resource for quantum computing.

To understand chaos in the quantum context, it is important to explore signatures of classical chaos in the deep quantum regime, where the standard Bohr correspondence principle cannot be invoked. A textbook model for studying quantum chaos is the quantum kicked top [10], which is a finite-dimensional spin system that displays chaotic dynamics in the classical limit. The quantum kicked top (QKT) has been extensively studied theoretically [22, 23, 24, 25, 26, 27, 28, 29]. The system can be described as a collection of indistinguishable qubits, which makes it attractive to explore in the framework of quantum information processing and NISQ devices. In the deep quantum regime, periodicities and symmetries in the two- and three-qubit QKT model were theoretically studied [29, 28]. A few experimental studies of the QKT have also been performed [14, 15, 16]. In [16], a 3-qubit model of the QKT was shown to exhibit ergodic dynamics and a resemblance between entanglement entropy and classical phase space dynamics was noted. Temporal periodicity and symmetries of the 2-qubit QKT were explored using NMR techniques in [14]. These experiments are limited to a small number of kicks due to decoherence times of the physical qubits. Furthermore, in these implementations the chaoticity parameter κ is determined by the strength and duration of interaction between the qubits, making it difficult to tune. To experimentally study the long term dynamics and dependence on κ rigorously, one needs to explore longer time scales and a wider range of κ . In this work, we show that mapping the QKT on to a programmable quantum circuit in a quantum computer allows simulations of the QKT that overcome previous experimental limitations. This opens new regimes of experimental exploration in both time and in parameter space.

We construct and demonstrate for the first time, an exact simulation of the 2-qubit quantum kicked top using a universal set of quantum logic gates. Our quantum circuit-based simulation is programmable and enables flexible initial state preparation and evolution. Using IBM’s 5-qubit chip *vigo*, we can prepare initial states and implement the dynamics of the QKT for an arbitrary number of kicks and a wide range of κ . The number of gates required for this simulation is independent of the number of kicks and value of κ . Therefore, our model does not suffer any systematic loss in fidelity with increasing number of kicks or κ values. Finally, full quantum state tomography enables us to explore signatures of chaos in 2-qubit entanglement.

The ability to vary κ and the number of kicks allows us to experimentally observe the periodic nature of the dynamics with respect to κ as well as kick number. Additionally, the temporal periodicity of the QKT can be used to obtain highly accurate time averages of relevant physical quantities. In particular, we explore the time-averaged entanglement for different initial spin coherent states (SCS). We find that a contour plot of the time average entanglement shows clear signatures of the classical phase space structures of regular islands in a chaotic sea, even in a deep quantum regime. We also show that the states initialized in chaotic regions of the phase space show intermediate values of average concurrence, whereas, the fixed points and the period-4 orbit correspond to the minimum and maximum values respectively. This behaviour is related to the degree of delocalization of the state and thus demonstrates a connection between delocalization and entanglement [30].

Our work shows that current quantum computers are useful for flexibly exploring new experimental regimes in quantum chaotic systems. Mapping the system onto a tunable quantum circuit lets us probe different aspects of the QKT dynamics without the need for building sophisticated customized hardware or being constrained by fixed system parameters. This method combines the ease of numerical simulation with the built-in quantum evolution of a physical system.

The paper is organized as follows: In section 2, the the quantum kicked top model is introduced and the chaotic classical limit is discussed. In section 3, our circuit-based approach and the mapping to the IBM *vigo* processor is described. In section 4, the experimental results of the IBM *vigo* simulations are discussed. Finally, conclusions, outlook and the scope of application of our circuit-based approach are discussed in section 5.

2 The quantum kicked top

The quantum kicked top (QKT) model was first introduced by Haake, Kus and, Scharf in 1987 [31]. It is now a widely studied model for exploring quantum chaos. The QKT is a time-dependent periodic spin system governed by the Hamiltonian

$$H = \hbar \frac{pJ_y}{\tau} + \hbar \frac{\kappa J_z^2}{2j} \left(\sum_{n=-\infty}^{n=\infty} \delta(t - n\tau) \right), \quad (1)$$

where J_x, J_y and J_z obey the standard angular momentum operator commutation relations. The operator $J^2 = J(J+1)\hbar^2$ commutes with the Hamiltonian and the magnitude of the angular momentum is a constant of motion. The Hamiltonian consists of a series of rotations (kicks) described by the J_y term alternating with torsion due to the non-linear J_z^2 term. τ is the duration between kicks, p is the angle of linear rotation in the y -direction, and κ is the strength of twist in the z -direction. The kick-to-kick Floquet time evolution operator can be written as

$$U = \exp\left(-i\frac{\kappa}{2j}J_z^2\right)\exp\left(-i\frac{p}{\tau}J_y\right). \quad (2)$$

The classical map for the kicked top can be obtained by writing the Heisenberg equations of motion for the angular momentum operators and then taking the limit $j \rightarrow \infty$. By defining the normalized variables $X = J_x/j$, $Y = J_y/j$ and $Z = J_z/j$, the classical equations of motions for $p=\pi/2$ are

$$\begin{aligned} X_{n+1}(\tau) &= Z_n(\tau)\cos(\kappa X_n(\tau)) + Y_n(\tau)\sin(\kappa X_n(\tau)), \\ Y_{n+1}(\tau) &= Y_n(\tau)\cos(\kappa X_n(\tau)) - Z_n(\tau)\sin(\kappa X_n(\tau)), \\ Z_{n+1}(\tau) &= -X_n(\tau) \end{aligned} \quad (3)$$

Here the dynamical variables (X, Y, Z) satisfy the constraint $X^2 + Y^2 + Z^2 = 1$, i.e., they are restricted to be on the unit sphere S^2 . Thus, the variables can be parameterized into spherical polar coordinates as $(X, Y, Z) = (\sin(\theta)\cos(\phi), \sin(\theta)\sin(\phi), \cos(\theta))$.

As the chaoticity parameter κ is varied, the classical dynamics ranges from regular motion (for $\kappa \leq 2.1$), to a mixture of regular and chaotic behaviour for different initial conditions (for $2.1 \leq \kappa \leq 4.4$), to fully chaotic motion (for $\kappa > 4.4$). The classical stroboscopic map (in spherical co-ordinates) for a range of initial conditions with $\kappa = 2.5$ and $\kappa = 3$ is plotted in Fig. 1a and Fig. 1b respectively.

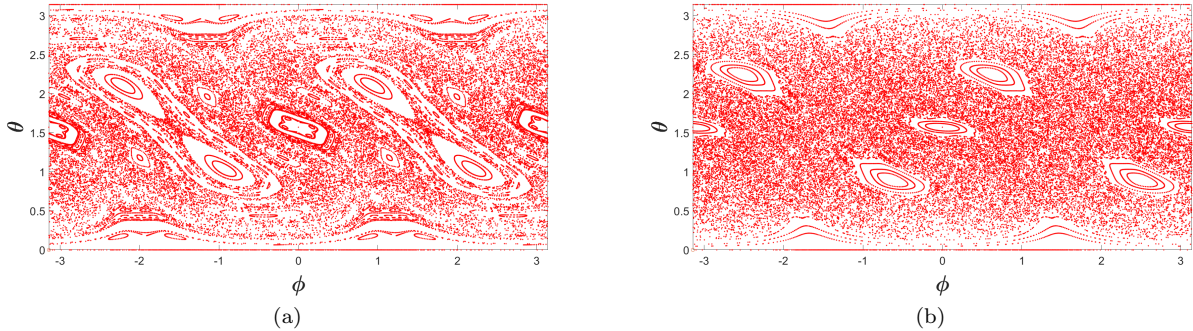


Figure 1: Stroboscopic map showing the classical time evolution over 150 kicks for **a.** $\kappa=2.5$ and **b.** $\kappa=3.0$ for 289 initial points in phase space.

3 Simulating quantum kicked top dynamics

3.1 Floquet operator

The time evolution of the system is described by evolving the initial state with the Floquet time evolution operator

$$U = \exp\left(-i\frac{\kappa}{2j}J_z^2\right)\exp(-ipJ_y). \quad (4)$$

Since $[H, J^2] = 0$ for the QKT Hamiltonian, it can be considered as an $N = 2j$ qubit system [30]. The spin- j operators are written in terms of the single qubit Pauli rotation operators as:

$$J_\alpha = \frac{1}{2} \sum_{i=1}^{2j} \sigma_{i\alpha}, \quad \alpha \in \{x, y, z\} \quad (5)$$

where $\sigma_{i\alpha}$ denotes σ_α acting on the i^{th} qubit. This allows us to rewrite the QKT Hamiltonian in $2j$ -qubit space:

$$H = \hbar \frac{\kappa}{8j} \left(2j + \sum_{\substack{i,k=1 \\ i \neq k}}^{2j} \sigma_{iz} \otimes \sigma_{kz} \right) \sum_{n=-\infty}^{\infty} \delta(t - n\tau) + \hbar \frac{p}{2\tau} \sum_{i=1}^{2j} \sigma_{iy}. \quad (6)$$

In particular, the $j = 1$ QKT is described by the 2-qubit Hamiltonian

$$H = \frac{\hbar k}{4} (\mathbb{I} + \sigma_z \otimes \sigma_z) \sum_n \delta(t - n\tau) + \frac{\hbar p}{2\tau} (\sigma_y \otimes \mathbb{I} + \mathbb{I} \otimes \sigma_y) \quad (7)$$

and, setting $\hbar = 1$, the corresponding single-kick time evolution unitary is

$$U = \exp \left(-i \frac{\kappa}{4} (\mathbb{I} + \sigma_z \otimes \sigma_z) \right) \exp \left(-i \frac{p}{2} (\sigma_y \otimes \mathbb{I} + \mathbb{I} \otimes \sigma_y) \right). \quad (8)$$

3.2 Initial States

Minimum uncertainty states in spin systems are spin coherent states (SCS) [32] that satisfy the uncertainty relation

$$\Delta J_i \Delta J_k = \frac{\hbar}{2} |\Delta J_l|, \quad (9)$$

where i, k and l are permutations of x,y and z. The uncertainty for these states is distributed symmetrically over the two operators. For larger j values, the SCS becomes highly localized around the point (θ, ϕ) in the phase space and hence in the classical limit of $j \rightarrow \infty$, approximates the classical angular momentum state located at (θ, ϕ) [10].

Spin squeezed states, which have asymmetric distribution of uncertainty, can display entanglement in the corresponding multi-qubit representation[33]. Since we are interested in studying entanglement that arises from the dynamics of the system, we choose SCSs as our initial states, thus ensuring there is no initial entanglement between the qubits. Given any point (θ, ϕ) in the classical phase space, we construct the corresponding SCS $|j; \theta, \phi\rangle$

$$|j; \theta, \phi\rangle = \exp[i\theta(J_x \sin \phi - J_y \cos \phi)] |j, j\rangle. \quad (10)$$

In the $2j$ -qubit space, we define our initial states as the SCSs

$$|j; \theta, \phi\rangle = |\theta, \phi\rangle^{\otimes 2j}, \quad (11)$$

where $|\theta, \phi\rangle$ are points on the Bloch sphere.

3.3 Implementation of unitaries with a quantum circuit

Any n -qubit unitary can be decomposed into $2^n(2^n - 1)/2$ single-qubit gates with controls. We follow the prescription in [34] to decompose our 2-qubit Floquet operator as

$$U = U_1 \times U_2 \times U_3 \times U_4 \times U_5 \times U_6, \quad (12)$$

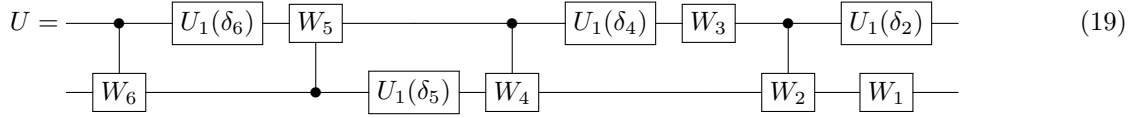
where U_i are either single-qubit unitaries or controlled unitaries of the form

$$U_i \equiv \begin{array}{c} \boxed{V_i} \\ | \\ \bullet \end{array} \text{ or } U_i \equiv \begin{array}{c} \bullet \\ | \\ \boxed{V_i} \end{array}.$$

In the circuit above, the two wires represent the two qubits, the solid dot represents the control qubit, and the box indicates the single qubit operation V_i on the target qubit. The exact decomposition for a 2-qubit gate in this scheme is

$$U = \begin{array}{c} \bullet \\ | \\ \boxed{V_5} \\ | \\ \bullet \end{array} \begin{array}{c} \bullet \\ | \\ \boxed{V_3} \\ | \\ \bullet \end{array} \begin{array}{c} \bullet \\ | \\ \boxed{V_2} \\ | \\ \bullet \end{array} \begin{array}{c} \bullet \\ | \\ \boxed{V_1} \\ | \\ \bullet \end{array} \begin{array}{c} \bullet \\ | \\ \boxed{V_6} \\ | \\ \bullet \end{array} \begin{array}{c} \bullet \\ | \\ \boxed{V_4} \\ | \\ \bullet \end{array} \begin{array}{c} \bullet \\ | \\ \boxed{V_2} \\ | \\ \bullet \end{array} \begin{array}{c} \bullet \\ | \\ \boxed{V_1} \\ | \\ \bullet \end{array} . \quad (13)$$

$W \in \text{SU}(2)$ is implemented as a U_3 gate and U_δ is implemented as $U_1(\delta)$. Hence, we obtain the final circuit decomposition for our 2-qubit Floquet operator on IBMQ:



with $W_i = U_3(\theta_i, \phi_i, \lambda_i)$.

Time evolution after multiple kicks is calculated by applying the Floquet unitary on the initial state repeatedly. This could be achieved by applying the set of gates given in Eq.19 consecutively N times to simulate evolution by N time steps. However, to mitigate the errors which may arise from the increasing number of gates, in our approach, we decompose the effective N -step unitary U^N using the same procedure as mentioned above. This means that the state after any arbitrary number of steps can be obtained by applying the same set of gates given in Eq. 19 with appropriate parameters. The advantage of this approach is that the number of gates is fixed and does not grow with the number of kicks. Similarly, time evolution for different values of κ can be implemented by computing the relevant parameters for the set of gates corresponding to the unitary $U^N(\kappa)$. This affords us a more fine-grained and flexible control over this parameter compared to other qubit-based realizations where the value of κ is set by tuning the time duration of interactions between the physical qubits.

After applying the appropriate set of gates to the initial states, the final states density matrix is constructed using state-tomography circuits built into Qiskit Ignis[37]. Physical quantities of interest can be calculated from this density matrix.

4 Exploring quantum chaos with a quantum computer

4.1 Performance of quantum simulations

Starting with various initial points for two different values of κ , we apply the quantum circuit for implementing N kicks on IBM *vigo*. We reconstruct the resulting final state by performing quantum state tomography and use the fidelity of the reconstructed state as a measure of simulation accuracy. For the theoretically predicted state ρ_{th} and the reconstructed state ρ_{vigo} , fidelity is given by $F(\rho_{\text{vigo}}, \rho_{\text{th}}) = (\text{tr}(\sqrt{\sqrt{\rho_{\text{th}}}\rho_{\text{vigo}}\sqrt{\rho_{\text{th}}}}))^2$. We observed that there is no systematic loss in fidelity with the number of kicks for different initial states and values of κ (Fig. 2). We can compute the average fidelity over different κ values in the range [0.5,6.5], and for different initial states as a function of time. As seen in Fig. 3, the average fidelities remain around 0.87.

To obtain a benchmark of how well our circuit method implemented on a publicly accessible quantum computer (IBM *vigo*) performs, we have compared the observed fidelities with that of previous QKT experiments[16], [14]. [16] reported monotonically decreasing fidelity with a low of 0.6 for 10 kicks. [14] reported a significant drop in fidelity from 6th to 8th kick with the lowest fidelity being 0.8. In our study, the non-decreasing trend in fidelity for much higher number of kicks can be attributed to the fixed number of gates for arbitrary number of kicks. By decomposing the unitary into elementary, programmable quantum gates, we effectively remove any constraints on the parameters of the physical system (QKT) that we can implement. In the IBM-Q systems, the error varies only with the number of single qubit physical rotations and CNOT gates [38] acting on each qubit. Since the number of gates in the circuit remains constant irrespective of the value of κ , we observe that the fidelity values do not depend on κ .

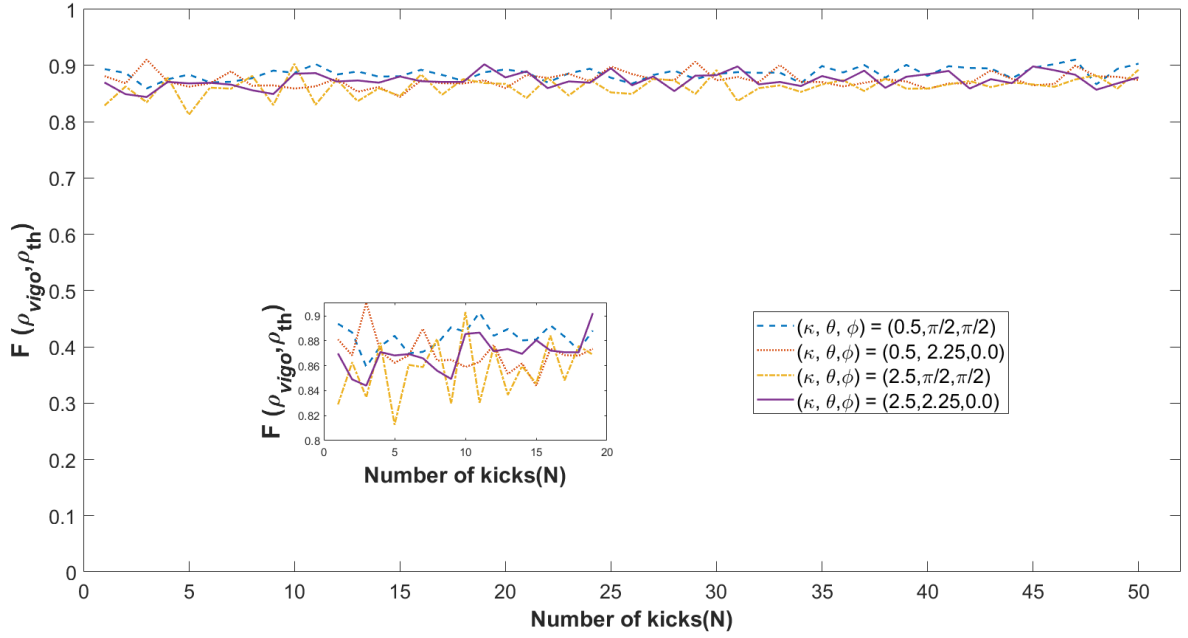


Figure 2: Fidelity of the tomographically reconstructed 2-qubit state for different initial states and different κ values on IBM *vigo*

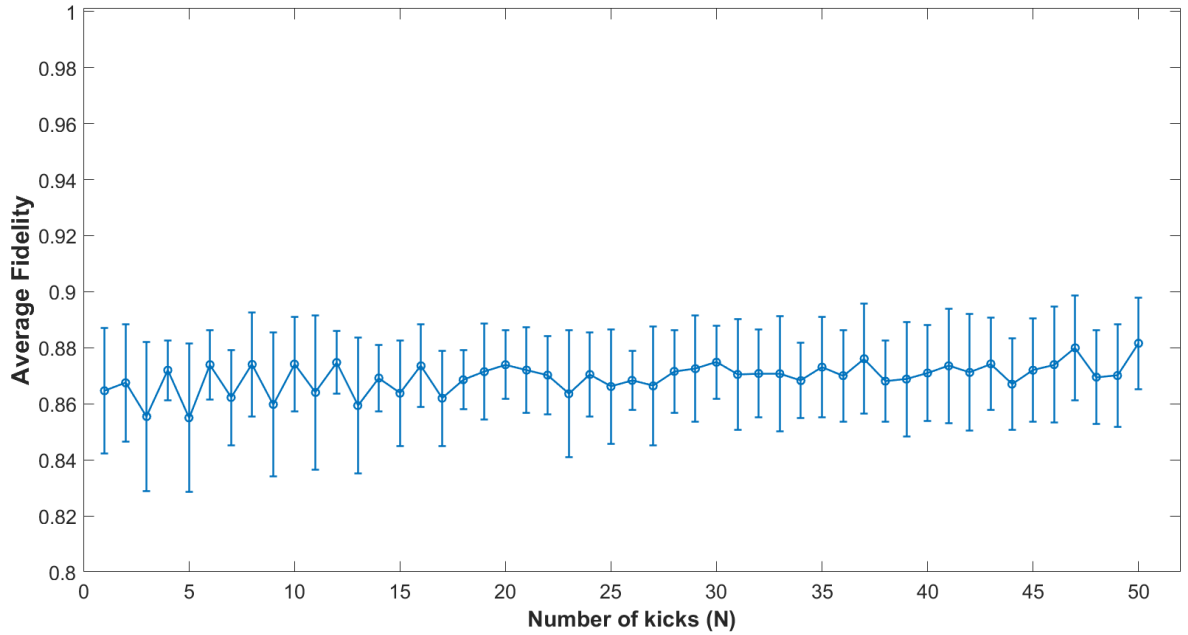


Figure 3: Fidelity of the tomographically reconstructed 2-qubit state averaged over initial states with $(\theta, \phi) \in \{(2.25, 0), (\pi/2, \pi/2), (\pi/2, 0)\}$ and $\kappa \in \{0.5, 2.5, 4.5, 6.5\}$ on IBM *vigo*. The error bars indicate standard deviation.

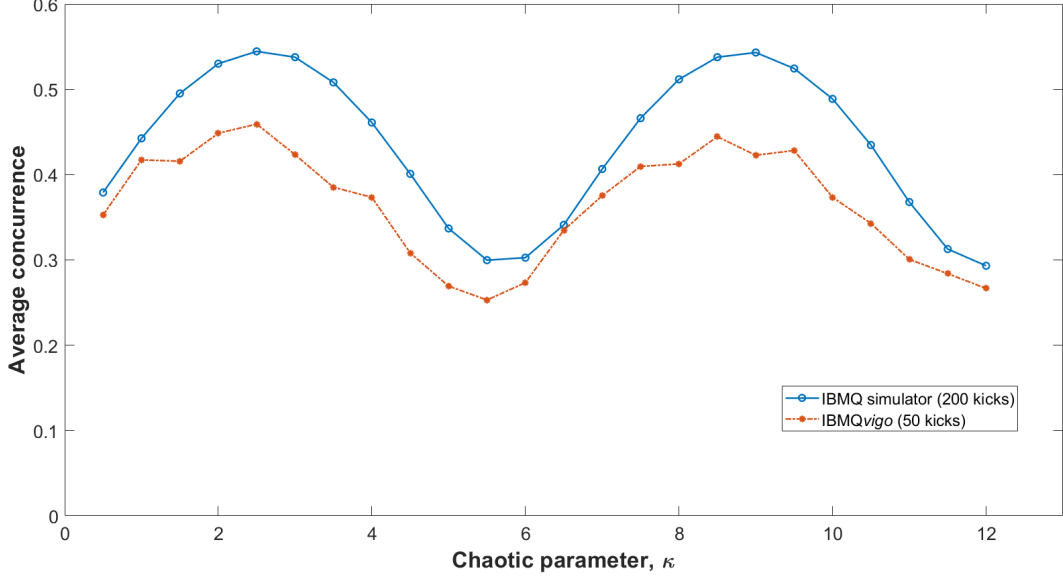


Figure 4: Time-averaged concurrence plotted against κ show a periodicity of 2π . The initial state is an SCS with $\theta = 2.25$ and $\phi = 2.0$. The average was taken over 200 steps for the simulated plot and over 50 steps on IBM *vigo*.

4.2 Observation of periodicity in κ

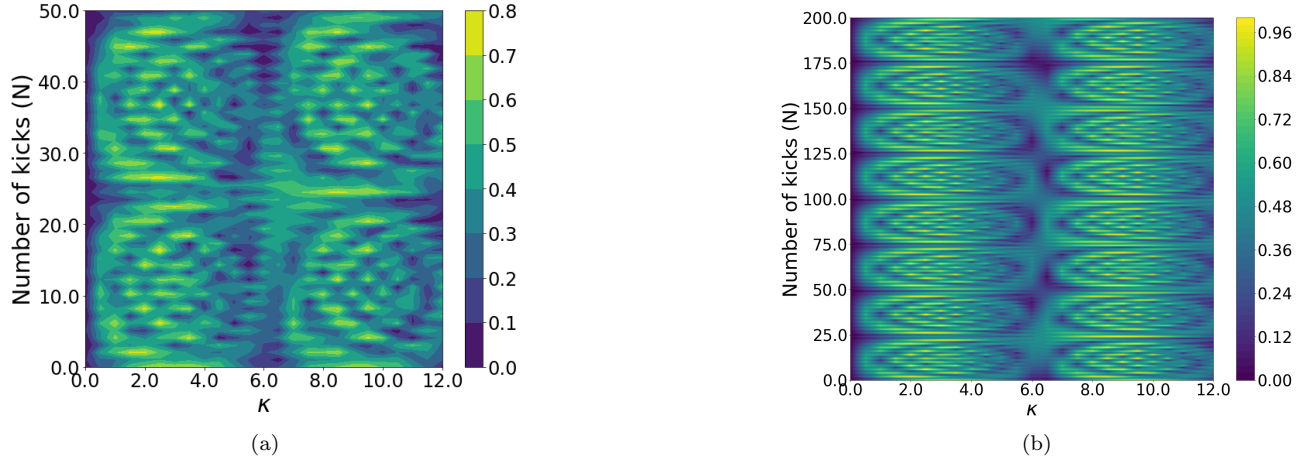


Figure 5: (a) Contour plot of concurrence over (a) 50 kicks for different values of κ on IBMQ *vigo* (b) 200 kicks for different values of kappa on IBMQ simulator. The initial state is an SCS with $\theta = 2.25$ and $\phi = 2.0$.

The ability to explore a wide range of values of the chaoticity parameter κ allows us to explore how chaos affects the dynamics. In particular, we study the effect of chaos (a classical phenomenon), on entanglement - a fundamentally quantum phenomenon. Here we consider the 2-qubit entanglement quantified by the concurrence as follows [39]. For a two-qubit density matrix ρ , the concurrence C is defined to be

$$C = \max(0, \sqrt{\lambda_1} - \sqrt{\lambda_2} - \sqrt{\lambda_3} - \sqrt{\lambda_4}), \quad (20)$$

where λ_i are eigenvalues of $\rho\tilde{\rho}$ such that $\lambda_4 \leq \lambda_3 \leq \lambda_2 \leq \lambda_1$ and $0 \leq C \leq 1$, and $\tilde{\rho} = \sigma_y \otimes \sigma_y \rho^* \sigma_y \otimes \sigma_y$ (where σ_y is Pauli matrix and ρ^* is complex conjugate of ρ in the standard basis). Concurrence is 0 for separable states

and 1 for the maximally entangled Bell states.

Figure 4 shows the time averaged 2-qubit concurrence as a function of κ for an initial SCS centered at $\theta = 2.25, \phi = 2.0$. The experimental results from the IBMQ hardware show good agreement with the output from the IBM quantum circuit simulator, and both show the periodic behaviour of κ . The period of 2π agrees with the theoretical prediction of $2\pi j$ [29]. To confirm the general periodicity of κ , we mapped the time evolution of the concurrence for 25 different values of κ ranging from 0 to 12 to create a contour plot (Fig. 5). The periodic nature of the dynamics can be observed in the concurrence as we scan over either the number of kicks or κ , while holding the other variable constant. The periodicity of quantum dynamics in the 2-qubit QKT model was explored experimentally in one previous NMR study [14], which considered four different values of κ and 8 kicks for each value of κ . Our work significantly expands the range of κ and the number of kicks explored, and directly connects the periodicity to the observed entanglement dynamics.

4.3 Entanglement and delocalization

The periodicity in the concurrence, combined with the ability to implement a high number of kicks, can be exploited to generate detailed average concurrence plots. By averaging over multiple periods of concurrence in the number of kicks, we can reduce the error in the value of average concurrence. This allows more detailed observations of signatures of chaos in entanglements dynamics.

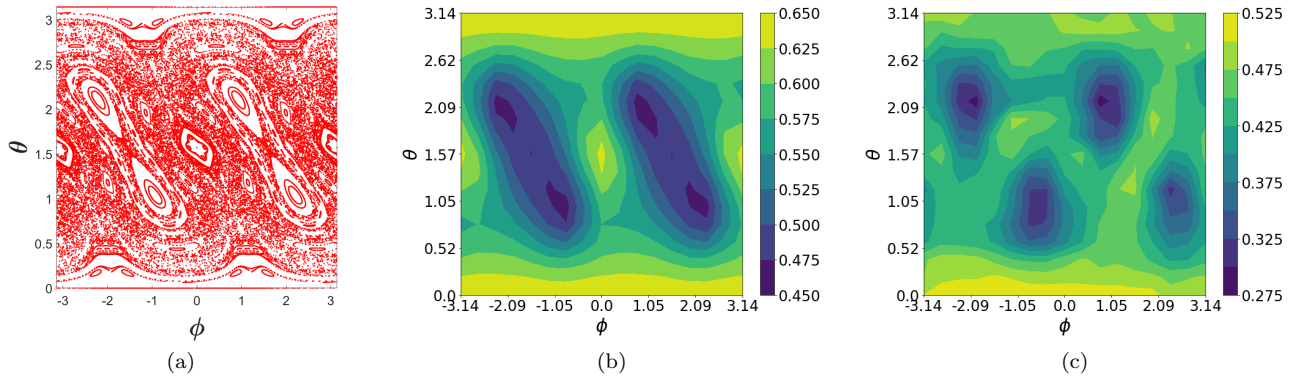


Figure 6: (a) Stroboscopic map, (b) average concurrence over 200 kicks on IBMQ simulator and (c) average concurrence over 50 kicks on IBMQ *vigo* for 289 initial points and $\kappa = 2.5$.

A contour plot of time-averaged concurrence as function of θ and ϕ for $\kappa = 2.5$ reflects the structures of the stroboscopic classical map as shown in Fig. 6. Furthermore, our plots have enough resolution to observe that the chaotic regions of the classical phase space show intermediate concurrence values. The four prominently visible islands of low concurrence correspond to fixed points of the classical dynamics. These islands are clearly distinguishable on the hardware plot and the left-right symmetry is maintained as shown in Fig. 6c. Points $(J_x/j, J_y/j, J_z/j) = (1, 0, 0), (0, 0, -1), (-1, 0, 0)$ and $(1, 0, 0)$, which constitute a period-4 orbit present in the classical dynamics of the system, show the highest values of average concurrence.

We note the correspondence between this trend in average concurrence and the degree of delocalization of various initial states after evolution with the Floquet unitary. This degree of delocalization [30] can be quantified by calculating the maximum overlap with respect to the set of minimum uncertainty spin coherent states.

$$O_{\text{SCS}}(|\psi(t)\rangle) = \max_{\text{SCS}} |\langle \text{SCS} | \psi(t) \rangle|. \quad (21)$$

Large values of O_{SCS} correspond to more localized states, as they indicate high overlap with spin coherent states. Delocalized states show low O_{SCS} values. The value of O_{SCS} for two different states, one in the high concurrence region and one in the low concurrence region are plotted against number of steps in Fig. 7, and show the connection between entanglement and delocalization. This is the first observation of this connection in the deepest quantum regime and confirms previous theoretical predictions [14],[28],[23].

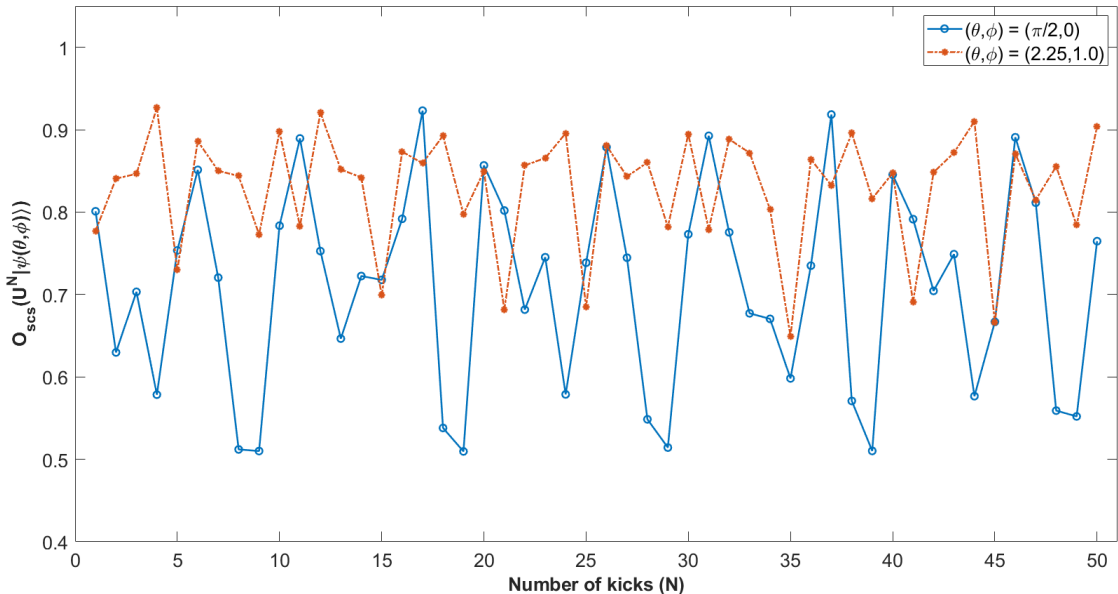


Figure 7: Evolution of O_{SCS} values for two different initial states for 50 kicks on on IBMQ *quito*. The evolution of initial state leading to higher concurrence $((\theta, \phi) = (\pi/2, 0))$ is more delocalized, i.e., has lower average O_{SCS} than that corresponding to lower concurrence $((\theta, \phi) = (2.25, 1))$.

5 Summary and discussion

In this work, we have proposed a quantum circuit-based approach to simulate and explore quantum chaos, and demonstrated its advantages over existing methods. The proposed method can be applied in general to any periodically driven finite dimensional quantum system. In our study, IBM’s 5-qubit open access quantum chip (*vigo*) was used as the experimental platform to implement the proposed approach for the 2-qubit quantum kicked top (QKT). The Hamiltonian of the QKT can be exactly expressed in terms of qubits since it is a finite-dimensional quantum system. Therefore, its evolution operator can be decomposed into quantum gates. Traditionally, experimental studies of quantum chaos have applied the same set of operations n times to explore time evolution. Here, we decomposed the unitary evolution operator for n kicks, U^n , into elementary quantum gates. This results in a fixed number of operations implementing the QKT evolution for any number of kicks. This hybrid combination of classical processing and quantum computing opens up the ability to perform high fidelity experimental studies of quantum chaos in new parameter regimes.

Since the value of the chaoticity parameter κ only determines the parameters of unitary rotations in the quantum circuit, and since the single qubit rotation errors are independent of the parameters, we were able to experimentally study chaotic dynamics over a wider range of κ and kick number compared to previous studies. By taking advantage of the high fidelity obtained for both a large number of kicks and arbitrary κ values, we experimentally demonstrated the periodicity of entanglement with time and κ with high accuracy. Our studies also clearly showed signature of chaos in the contour plot of average 2-qubit concurrence despite being in the deeply quantum regime. Furthermore, we reported the first observation of the correspondence between average entanglement and delocalization in the 2-qubit QKT.

Our results demonstrate the advantages of circuit-based NISQ devices for exploring fundamental questions in quantum information and quantum chaos despite their noise and scale limitations. Previous studies [20],[21] have noted that chaos could influence the efficient and stable operation of quantum computers. In [40], it was shown that chaos affects the balance between the disorder that maintains the stability of qubits and nonlinear resonator couplings that is used to manipulate interactions. This plays an integral role in future transmon device engineering. The gate-based circuit model of QKT can be used as an efficient tool for studying these effects in different situations.

Acknowledgements

We thank M. Kumari, R. Mann, A. Mashatan and N. Lutkenhaus for useful discussions. This work was supported by the Natural Sciences and Engineering Research Council of Canada. Wilfrid Laurier University is located in the traditional territory of the Neutral, Anishnawbe and Haudenosaunee peoples. We thank them for allowing us to conduct this research on their land.

References

- [1] J. Ignacio Cirac and Peter Zoller. “Goals and opportunities in quantum simulation”. In: *Nature Physics* 8.4 (Apr. 2012), pp. 264–266. DOI: [10.1038/nphys2275](https://doi.org/10.1038/nphys2275). URL: <http://dx.doi.org/10.1038/nphys2275>.
- [2] Ehud Altman et al. “Quantum Simulators: Architectures and Opportunities”. In: *PRX Quantum* 2.1 (Feb. 2021). DOI: [10.1103/prxquantum.2.017003](https://doi.org/10.1103/prxquantum.2.017003). URL: <http://dx.doi.org/10.1103/PRXQuantum.2.017003>.
- [3] Richard P. Feynman. “Quantum mechanical computers”. In: *Foundations of Physics* 16.6 (June 1986), pp. 507–531. DOI: [10.1007/bf01886518](https://doi.org/10.1007/bf01886518). URL: <http://dx.doi.org/10.1007/BF01886518>.
- [4] “Simulating molecules on a cloud-based 5-qubit IBM-Q universal quantum computer”. In: 4 (). DOI: [10.1038/s42005-021-00616-1](https://doi.org/10.1038/s42005-021-00616-1). URL: <http://dx.doi.org/10.1038/s42005-021-00616-1>.
- [5] “IBM Q Experience as a versatile experimental testbed for simulating open quantum systems”. In: 6 (). DOI: [10.1038/s41534-019-0235-y](https://doi.org/10.1038/s41534-019-0235-y). URL: <http://dx.doi.org/10.1038/s41534-019-0235-y>.
- [6] I. M. Georgescu, S. Ashhab, and Franco Nori. “Quantum simulation”. In: *Rev. Mod. Phys.* 86 (1 Mar. 2014), pp. 153–185. DOI: [10.1103/RevModPhys.86.153](https://doi.org/10.1103/RevModPhys.86.153). URL: <https://link.aps.org/doi/10.1103/RevModPhys.86.153>.
- [7] “Quantum Computing in the NISQ era and beyond”. In: 2 (). DOI: [10.22331/q-2018-08-06-79](https://doi.org/10.22331/q-2018-08-06-79). URL: <http://dx.doi.org/10.22331/q-2018-08-06-79>.
- [8] Sam McArdle et al. “Quantum computational chemistry”. In: *Reviews of Modern Physics* 92.1 (Mar. 2020). DOI: [10.1103/revmodphys.92.015003](https://doi.org/10.1103/revmodphys.92.015003). URL: <http://dx.doi.org/10.1103/RevModPhys.92.015003>.
- [9] Wojciech Hubert Zurek and Juan Pablo Paz. “Quantum chaos: a decoherent definition”. In: *Physica D: Nonlinear Phenomena* 83.1–3 (May 1995), pp. 300–308. DOI: [10.1016/0167-2789\(94\)00271-q](https://doi.org/10.1016/0167-2789(94)00271-q). URL: [http://dx.doi.org/10.1016/0167-2789\(94\)00271-q](http://dx.doi.org/10.1016/0167-2789(94)00271-q).
- [10] F. Haake, M. Kuś, and R. Scharf. “Classical and quantum chaos for a kicked top”. In: *Zeitschrift für Physik B Condensed Matter* 65 (Sept. 1987), pp. 381–395. DOI: [10.1007/bf01303727](https://doi.org/10.1007/bf01303727). (Visited on 01/07/2021).
- [11] Fritz Haake. “Quantum signatures of chaos”. In: *Quantum Coherence in Mesoscopic Systems*. Springer, 1991, pp. 583–595.
- [12] Jun Li et al. “Measuring Out-of-Time-Order Correlators on a Nuclear Magnetic Resonance Quantum Simulator”. In: *Physical Review X* 7.3 (July 2017). DOI: [10.1103/physrevx.7.031011](https://doi.org/10.1103/physrevx.7.031011). URL: <http://dx.doi.org/10.1103/PhysRevX.7.031011>.
- [13] Pascal Szriftgiser et al. “Experimental study of quantum chaos with cold atoms”. In: *Communications in Nonlinear Science and Numerical Simulation* 8.3–4 (Sept. 2003), pp. 301–313. DOI: [10.1016/S1007-5704\(03\)00031-5](https://doi.org/10.1016/S1007-5704(03)00031-5). URL: [http://dx.doi.org/10.1016/S1007-5704\(03\)00031-5](http://dx.doi.org/10.1016/S1007-5704(03)00031-5).
- [14] V. R. Krithika et al. “NMR studies of quantum chaos in a two-qubit kicked top”. In: *Phys. Rev. E* 99 (3 Mar. 2019), p. 032219. DOI: [10.1103/PhysRevE.99.032219](https://doi.org/10.1103/PhysRevE.99.032219). URL: <https://link.aps.org/doi/10.1103/PhysRevE.99.032219>.
- [15] S Chaudhury et al. “Quantum signatures of chaos in a kicked top”. In: *Nature* 461.7265 (2009), pp. 768–771.
- [16] C Neill et al. “Ergodic dynamics and thermalization in an isolated quantum system”. In: *Nature Physics* 12.11 (2016), pp. 1037–1041.
- [17] Malcolm C. Smith. “The general problem of the stability of motion : Translated and Edited by A. T. Fuller. Taylor and Francis, 1992”. In: *Autom.* 31 (1995), pp. 353–354.
- [18] Edward Ott. *Chaos in Dynamical Systems*. Aug. 2002. DOI: [10.1017/cbo9780511803260](https://doi.org/10.1017/cbo9780511803260). URL: <http://dx.doi.org/10.1017/CB09780511803260>.

- [19] BISWA NATH DATTA. “STABILITY, INERTIA, AND ROBUST STABILITY”. In: *Numerical Methods for Linear Control Systems*. Elsevier, 2004, pp. 201–243. DOI: [10.1016/B978-012203590-6/50011-2](https://doi.org/10.1016/B978-012203590-6/50011-2). URL: <http://dx.doi.org/10.1016/B978-012203590-6/50011-2>.
- [20] B. Georgeot and D. L. Shepelyansky. “Quantum chaos border for quantum computing”. In: *Phys. Rev. E* 62 (3 Sept. 2000), pp. 3504–3507. DOI: [10.1103/PhysRevE.62.3504](https://doi.org/10.1103/PhysRevE.62.3504). URL: <https://link.aps.org/doi/10.1103/PhysRevE.62.3504>.
- [21] B. Georgeot and D. L. Shepelyansky. “Emergence of quantum chaos in the quantum computer core and how to manage it”. In: *Phys. Rev. E* 62 (5 Nov. 2000), pp. 6366–6375. DOI: [10.1103/PhysRevE.62.6366](https://doi.org/10.1103/PhysRevE.62.6366). URL: <https://link.aps.org/doi/10.1103/PhysRevE.62.6366>.
- [22] Vaibhav Madhok et al. “Signatures of chaos in the dynamics of quantum discord”. In: *Phys. Rev. E* 91 (3 Mar. 2015), p. 032906. DOI: [10.1103/PhysRevE.91.032906](https://doi.org/10.1103/PhysRevE.91.032906). URL: <https://link.aps.org/doi/10.1103/PhysRevE.91.032906>.
- [23] Vaibhav Madhok, Shruti Dogra, and Arul Lakshminarayan. “Quantum correlations as probes of chaos and ergodicity”. In: *Optics Communications* 420 (6 Aug. 2018), pp. 189–193. DOI: [10.1103/PhysRevE.99.062217](https://doi.org/10.1103/PhysRevE.99.062217). URL: <https://doi.org/10.1016/j.optcom.2018.03.069>.
- [24] Xiaoguang Wang et al. “Entanglement as a signature of quantum chaos”. In: *Physical Review E* 70.1 (2004), p. 016217.
- [25] C. R. Paul S. Ghose and R. Stock. “Quantum Chaos and Tunneling in the Kicked Top”. In: *laser Physics* 18 (9 Sept. 2007), pp. 1098–1105. DOI: [10.1134/S1054660X0809017X](https://doi.org/10.1134/S1054660X0809017X). URL: <https://doi.org/10.1134/S1054660X0809017X>.
- [26] Shohini Ghose and Barry Sanders. “Entanglement dynamics in chaotic system”. In: *Phys. Rev. A* 70 (6 Dec. 2004), p. 062315. DOI: [10.1103/PhysRevA.70.062315](https://doi.org/10.1103/PhysRevA.70.062315). URL: <https://doi.org/10.1103/PhysRevA.70.062315>.
- [27] Shohini Ghose et al. “Chaos, entanglement, and decoherence in the quantum kicked top”. In: *Physical Review A* 78.4 (2008), p. 042318.
- [28] Joshua B Ruebeck, Jie Lin, and Arjendu K Pattanayak. “Entanglement and its relationship to classical dynamics”. In: *Physical Review E* 95.6 (2017), p. 062222.
- [29] Udaysinh T. Bhosale and M. S. Santhanam. “Periodicity of quantum correlations in the quantum kicked top”. In: *Phys. Rev. E* 98 (5 Nov. 2018), p. 052228. DOI: [10.1103/PhysRevE.98.052228](https://doi.org/10.1103/PhysRevE.98.052228). URL: <https://link.aps.org/doi/10.1103/PhysRevE.98.052228>.
- [30] Meenu Kumari. “Quantum-Classical Correspondence and Entanglement in Periodically Driven Spin Systems”. In: *Uwaterloo.ca* (July 2019). DOI: <http://hdl.handle.net/10012/14860>. URL: <https://uwspace.uwaterloo.ca/handle/10012/14860>.
- [31] Fritz Haake, M Kuś, and Rainer Scharf. “Classical and quantum chaos for a kicked top”. In: *Zeitschrift für Physik B Condensed Matter* 65.3 (1987), pp. 381–395.
- [32] J M Radcliffe. “Some properties of coherent spin states”. In: *Journal of Physics A: General Physics* 4 (May 1971), pp. 313–323. DOI: [10.1088/0305-4470/4/3/009](https://doi.org/10.1088/0305-4470/4/3/009). (Visited on 06/19/2020).
- [33] Jian Ma et al. “Quantum spin squeezing”. In: *Physics Reports* 509 (Dec. 2011), pp. 89–165. DOI: [10.1016/j.physrep.2011.08.003](https://doi.org/10.1016/j.physrep.2011.08.003). (Visited on 01/07/2021).
- [34] Chi-Kwong Li and Diane Pelejo. “Decomposition of quantum gates”. In: *arXiv:1311.3599 [quant-ph]* (Dec. 2013). URL: <https://arxiv.org/abs/1311.3599> (visited on 01/07/2021).
- [35] IBM Quantum team. Retrieved from [ibmq_vigo v1.0.2](https://quantum-computing.ibm.com) (2020). URL: <https://quantum-computing.ibm.com>.
- [36] *Qiskit 0.23.2 documentation — Qiskit 0.23.2 documentation*. qiskit.org. URL: <https://qiskit.org/documentation/index.html> (visited on 01/07/2021).
- [37] *Qiskit: An Open-source Framework for Quantum Computing*. DOI: [10.5281/ZENODO.2562111](https://doi.org/10.5281/ZENODO.2562111). URL: <https://zenodo.org/record/2562111>.
- [38] Shin Nishio et al. “Extracting Success from IBM’s 20-Qubit Machines Using Error-Aware Compilation”. In: *ACM Journal on Emerging Technologies in Computing Systems* 16 (July 2020), pp. 1–25. DOI: [10.1145/3386162](https://doi.org/10.1145/3386162). URL: <https://arxiv.org/abs/1903.10963> (visited on 07/13/2021).

- [39] William K. Wootters. “Entanglement of Formation of an Arbitrary State of Two Qubits”. In: *Phys. Rev. Lett.* 80 (10 Mar. 1998), pp. 2245–2248. DOI: [10.1103/PhysRevLett.80.2245](https://doi.org/10.1103/PhysRevLett.80.2245). URL: <https://link.aps.org/doi/10.1103/PhysRevLett.80.2245>.
- [40] C. Berke et al. “Transmon platform for quantum computing challenged by chaotic fluctuations”. In: *arXiv: Quantum Physics* (2020).